Chapter 4
Rockslide and Rock Avalanche Dams in the Southern Alps, New Zealand

O. Korup

1 Introduction

Studying the blockage of mountain rivers by bedrock landslides offers both fascinating and challenging prospects. It allows us to investigate not only some of the largest processes of mass movement on the Earth surface, but also the fluvial response to the emplacement of many millions of tons of rock and debris. The decay process of river-blocking debris links geomorphology to hazard and risk assessment, given the potential for catastrophic outburst floods and debris flows from rockslide-dammed lakes [26].

There is a steadily growing number of studies on landslide dams in high mountain belts throughout the world [4, 16]. In New Zealand, the occurrence of landslide dams is regionally clustered and largely controlled by relief, lithology, and landslide trigger mechanisms [24]. Landslide dams were mainly mapped in the East Cape, Taranaki, and Wanganui regions of North Island, and the Southern Alps and Fiordland mountains of South Island [17]. This pattern is partly an artefact of the regional landslide-triggering effect of historic earthquakes.

This study is intended to give a state-of-the-art overview on natural dams formed by large rockslides and rock avalanches in the Southern Alps of New Zealand. The term "large" refers here to an arbitrarily defined threshold of a mobilised volume $>10^6$ m^3. This contribution augments and updates previous seminal studies [24, 30]. Geomorphic evidence from various sources is presented and analysed with respect to blockage type, geomorphometric characteristics, distribution, post-failure morphodynamics, and fluvial adjustment. The discussion focuses on constraints on blockage types, regional and global comparison, trigger mechanisms, dam longevity, geomorphic long-range and long-term effects, as well as some hazard and risk implications. Other recent research issues on landslide dams in New Zealand were reviewed earlier [16].

O. Korup (✉)
Institute of Earth and Environmental Sciences, University of Potsdam,
D-14776 Potsdam, Germany
e-mail: oliver.korup@geo.uni-potsdam.de

S.G. Evans et al. (eds.), *Natural and Artificial Rockslide Dams*, Lecture Notes in Earth Sciences 133, DOI 10.1007/978-3-642-04764-0_4,

2 The Southern Alps of New Zealand

The geomorphic setting of the Southern Alps results from the close coupling of tectonic uplift and erosion, creating a mountain range asymmetric in cross-section [15, 31]. Dextral transpression along the Alpine Fault, which marks the Australian-Pacific plate boundary through the South Island of New Zealand, rapidly exhumes partially metamorphic mid-late Triassic greywacke of the Torlesse Terrane along a ramp-like structure [20]. The resulting mountain range attains elevations up to nearly 3,700 m a.s.l. with deeply dissected valleys. A major backthrust structure is evident in the Main Divide Fault Zone along the topographic backbone of the Southern Alps, and major alpine valleys adapted to the course of numerous oblique reverse, normal, and strike-slip faults [21]. Uplift and erosion rates vary throughout the Southern Alps and are highest at <11 mm/year near the Alpine Fault, and lowest in the east at ~1 mm/year [23, 27]. Metamorphic overprint on greywacke is exposed in NW-ward increasing grade, attaining amphibolite schist facies at the Alpine Fault, whereas subgreenschist and unaltered greywacke/argillite facies dominate east of the divide. The southwestern fringe of the Southern Alps is characterised by accreted and fault-bended terranes, including rocks of ultramafic lithology [23].

The mountain belt acts as a barrier to moisture-bearing winds from the Tasman Sea, causing orographically-enhanced precipitation of up to 14 m/year west of the main divide [13]. During the Quaternary, the Southern Alps were subject to numerous glaciations, and the terminal moraines of valley glaciers on the western fringe were drowned by postglacial sea-level rise. Based on physiographic characteristics, the Southern Alps can be divided into a Western (WSA), Axial (ASA), and Eastern (ESA) part [31]. Valleys in the WSA are generally steep, V-shaped, closely spaced, and rejuvenated by coseismic base-level changes along the Alpine Fault. The ASA have the highest elevations and are dominated by glacial landforms. In the ESA, basin areas are generally larger, and tributaries feed into broad moraine-fringed valley trains, which retain extensive amounts of glacigenic deposits and large ice-scoured intramontane lake basins (Fig. 4.1).

Fluvial sediment yields vary between 10^4 and 10^2 t/km^2/year, west and east of the main divide, respectively [9]. The contemporary regional sediment yield from the WSA makes up 30% of the total export from the New Zealand land mass [14].

Important predisposing factors for rock-slope instability in the study area include gravitational stress, deterioration of rock-mass strength through repeated earthquake shaking, hanging-wall shattering, and incision-driven loss of lateral support. The term "rockslide" is used here in a general sense, and comprises slope failures in bedrock, involving an arbitrary minimum volume of 10^6 m^3 of translational/rotational sliding, toppling, or other types of deep-seated slope deformation. The term "rock avalanche" is used in its strict sense, and refers to large volumes (>10^6 m^3) of fragmenting rock particles in extremely rapid flow movement [6].

Trigger mechanisms include seismic ground shaking, high-intensity rainstorms, and fluvial undercutting. Several historic rock avalanches have occurred without

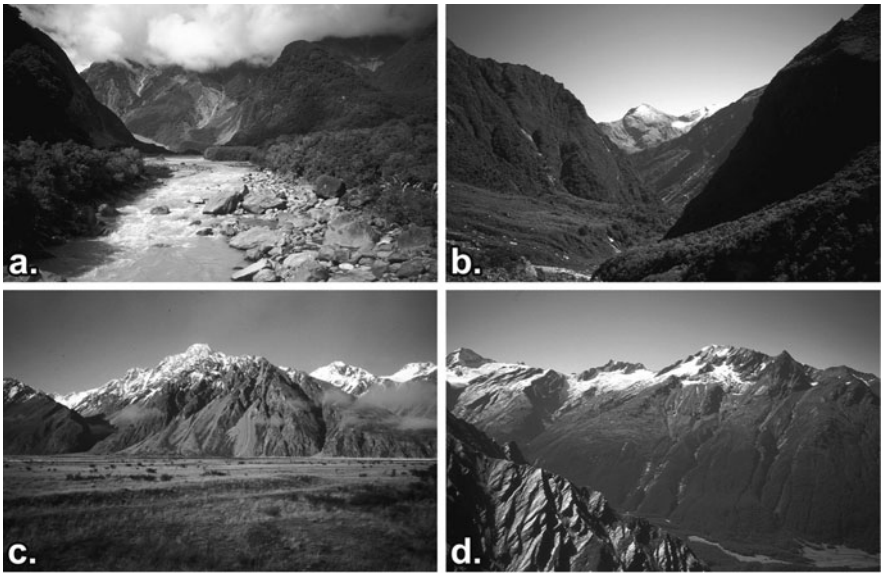

Fig. 4.1 Typical valley geometries of the Southern Alps, New Zealand (**a**) Glacial trough valley, lower Fox River, WSA; (**b**) Fluvially-incised V-shaped valley near the main divide, upper Copland River, WSA; (**c**) Extensive valley train fringed by debris-mantled slopes, Tasman River, Mt Cook, ASA; (**d**) Alpine valley walls developed in Otago Schist, West Matukituki River, ESA

any observed triggers and may have resulted from exceedance of intrinsic stress thresholds, possibly representing the catastrophic culmination of rock creep [22]. Very large rock avalanches can be caused by $M > 6.5$ earthquakes, on slopes >25°, and >100 m high, and especially on strongly shaken high narrow ridges [12].

Significant ($M \geq 5.5$) historic earthquakes in the study area occurred near Arthur's Pass, ASA, in 1929 and 1995. Large ($M \sim 8$) prehistoric (i.e., pre-1850 in New Zealand) earthquakes along the Alpine Fault were inferred from several palaeoseismological studies to occur every 250–300 year on average [2, 29].

Regional studies on landslides and landslide dams in the Southern Alps [1] and New Zealand [24], augmented with new case studies and results from geomorphometric analyses [17], were major sources for this compilation. There are currently 52 documented rock avalanches ($>10^6$ m^3) in the Southern Alps, several of which also had dammed ephemeral lakes [22, 30]. Few further studies addressed the consequences of rockslide and rock avalanche dams in the region. Recently, landslide dam-break failures were addressed in quantitative hazard and risk assessments for Franz Josef Glacier Township, an increasingly popular tourist destination at the fringe of the WSA [5, 7]. Finally, sediment budgets indicate extreme debris discharge from historic rockslides and described geomorphic off-site consequences for downstream reaches [19].

3 Rockslide and Rock Avalanche Dams in the Southern Alps

3.1 Identification and Compilation

The study area covers some 15,000 km^2 of mountainous terrain between 168 and 172°E, and 42° 30′–44° 30′S. Its northern and southern boundaries roughly coincide with the Alpine Fault trace in the Taramakau valley and a line from the upper Cascade River to Lake Wanaka, respectively. The western and eastern boundaries are defined by the Westland piedmont and Lakes Pukaki and Tekapo, respectively (Fig. 4.2). The locations and geomorphic characteristics of 43 rockslide and rock avalanche dams are part of a national inventory of over 240 landslide dams compiled from various sources [1, 12, 17, 24]. More than half of all recorded landslide dams in New Zealand were formed by large rock-slope failures, with most of them occurring in the Southern Alps and adjacent Fiordland. Almost 30% of all recorded landslide dams in New Zealand were formed by rock avalanches [17].

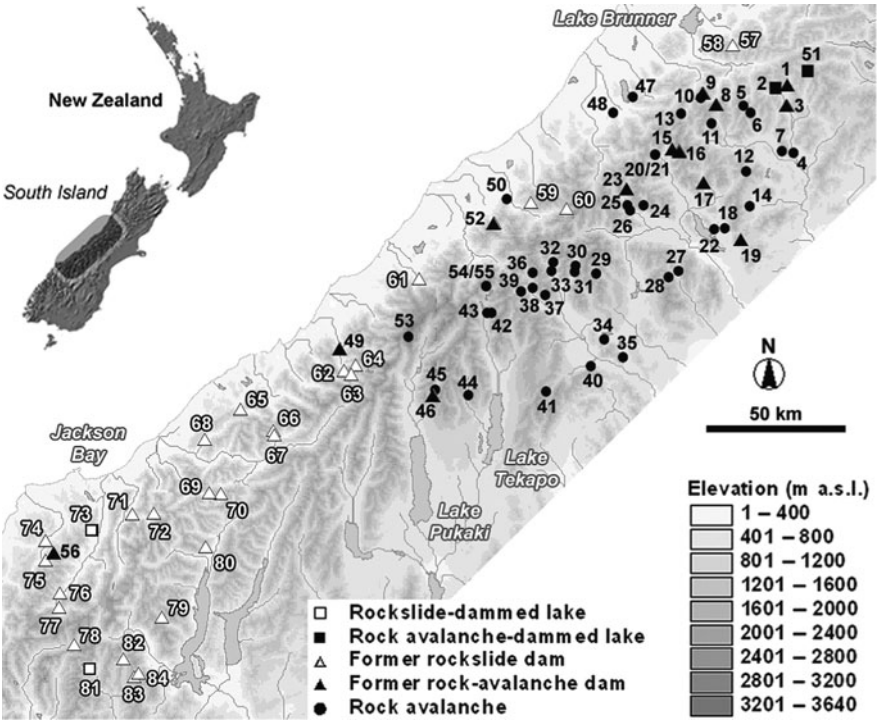

Fig. 4.2 Map showing the distribution of 43 rockslide (△, □) and rock avalanche dams (▲, ■) in the Southern Alps, New Zealand. Numbers refer to rock avalanche (*black*) and rockslide (*white*) locations, including all rock avalanches >10^6 m^3 (●) currently reported. Selected sites are described in Table 4.1. Note that previously reported rock avalanches [30] retain their original numbering. Mean density is 0.003 dams/km^2

Table 4.1 Characteristics of selected rockslide and rock avalanche dams in the Southern Alps, New Zealand. Numbers (#) refer to locations in Fig. 4.2. V_L = deposit volume; H_D = dam height; L_D = dam length; W_D = dam width; A_C = contributing catchment area

#	Location	Type[a]	V_L (10^6 m^3)	H_D (m)	L_D (km)	W_D (km)	A_C (km^2)	Remarks
23	Boundary Ck	Ra (II) E	280	80	1.3	2.6	55	H_D max. 110 m
16	Burnett Str	Ra (II) E	7	30	0.3	0.5	12	H_D max. 40 m
3	Casey Hut	Ra (III) E	23	10	–	–	161	
78	Dart Hut	Rs (II) E	>22	–	–	0.4	49	episodic failures
51	Ellis Str	Ra (II) E	5	5	–	–	2	
83	Harris (Pt 1845)	Rs (II) E	8	30	0.2	0.8	3	
84	Harris (Pt 1870)	Rs (II) E	–	–	–	1.1	7	
46	Jollie	Ra (III) E	77	50	1.0	1.1	86	H_D max. 60 m
81	Lochnagar	Rs (II) L	690	340	2.1	2.0	21	H_D max. 400 m
79	Minaret Burn	Rs (II) E	25		0.3	1.2	30	
2	Minchin	Ra (II) L	27	150	0.6	0.8	25	
82	Polnoon Burn	Rs (II) E	140	120	1.2	1.5	32	H_D max. 140 m
1	Thompson Str	Ra (II) E	18	40	0.6	0.7	37	
80	Tiel Ck	Crs (II) E	36	–	0.3	1.2	24	
17	Triangle Ck	Ra (II) E	60	50	1.1	1.6	105	H_D max. 110 m
15	Weka Str	Ra (II) E	19	–	–	–	4	
59	Carls Ridge	Crs (II) E	25	20	0.1	0.4	3	debris-flow dam
72	Crevice Gorge	Rs (II) E	–	90	0.4	0.7	25	
57	Crooked A	Crs (VI) E	170	20	0.3	1.2	38	
58	Crooked B	Rs (VI) E	40	20	–	1.0	38	
62	Dirty Ck	Rs (II) E	–	–	0.5	1.8	43	exact size unknown
64	Douglas	Wrs (II) E	14	50	0.8	0.9	60	120-m deep gorge
75	Falls Ck	Rs (III) E	130	50	–	1.5	22	
74	Hope Blue R.	Rs (III) E	>130	200	1.8	2.6	177	200-m deep gorge
70	Howe Ck	Rs (II) E	5	–	0.2	0.6	24	
9	Hunts Ck	Ra (III) E	35	40	–	–	11	
63	Lame Duck Flat	Rs (II) E	62	–	–	1.0	38	
77	McArthurs Flat	Rs (II) E	45	–	0.3	1.0	179	

Table 4.1 (continued)

#	Location	Type[a]	V_L (10^6 m^3)	H_D (m)	L_D (km)	W_D (km)	A_C (km^2)	Remarks
56	McKay Ck	Ra (III) E	–	100	–	0.8	10	
52	Poerua	Ra (III) E	10–15	120	0.5	0.7	50	
69	Princes Ck	Rs (II) E	50	–	–	1.6	3	
71	Te Naihi	Rs (II) E	–	30	0.5	1.0	76	rapids at breach site
60	Whirlwind Spur	Rs (II) E	–	–	0.2	1.4	12	
66	Zeilian Ck A	Rs (II) E	8	–	–	1.0	13	
67	Zeilian Ck B	Rs (VI) E	–	–	–	1.2	23	
8	Zig–Zag	Ra (III) E	43	100	–	1.4	15	H_D max. 130 m

[a]Dam type [2] in brackets, E = partly eroded, L = presently retains lake; Ra = rock avalanche; Rs = rockslide; Crs = complex rock slide; Wrs = wedge failure/rock slide.

Many of the Southern Alps headwaters show ample evidence of channel diversion and short-lived blockage in response to lateral debris input from landslides and steep tributary streams. Key geomorphic indications of rockslide and rock avalanche dams chiefly comprise amphitheatre-shaped, often scree-mantled, detachment scars with associated extensive hummocky, furrowed, and blocky deposits covering the valley floor [30].

Conspicuous changes in channel pattern and morphology limited to rockslide and rock avalanche deposits or their adjacent reaches are further diagnostic landforms. Non-catastrophic rock-slope deformation was identified by tensional scarp depressions, bulging (toe) slopes, or conspicuous lack of fluvial dissection. Often, place names such as "Rotten Ridge" (Roaring Swine Ck, Haast River), "Trembling Spur", or "Seismic Rift" (Palmer Ck, Waiatoto River) also indicate potential sites of rock-slope instability.

Several large rockslides occur at tributary junctions. There, enhanced downcutting following base-level adjustments and debuttressing along two oblique erosional fronts may favour dilatational slope movement.

Size estimates of rockslides and rock avalanches are expressed as volume of displaced material, V_L, or total affected area, A_L (scarp and deposit), allowing for an average error of $\pm 30\%$. Rockslide and rock avalanche dam height, H_D, was estimated from interpolating river longitudinal profiles along the blockage site, and the elevation difference between the deposit top and the present river bed. A measurement error of $\pm 15\%$ was assumed, due to often quite substantial differences between maximum and minimum elevations on top of rockslide and rock avalanche dams relative to the (breach-) channel bed.

The maximum width and length of rockslide and rock avalanche dams, W_D and L_D, respectively, were estimated with an accuracy of ± 100 m from geomorphic sketches, air photos, topographic maps, and digital elevation models. Dense vegetation cover – particularly in the WSA – as well as unquantified erosion and deposition following dam formation made the accurate reconstruction of some dam geometries difficult. In many cases, the size of dams and formerly dammed lakes requires further validation and reconstruction from field evidence. Thus, certain characteristics of rockslide and rock avalanche dams are not equally available, so that mostly sub-sets of the database can be compared (Table 4.1).

Data presented here include do not include minor (<0.02 km^2) rockslide ponds perched on top of the Thomson Range rock-mass collapse, Arawhata River (#73, Fig. 4.2), or the 1929 Falling Mountain rock avalanche, Otehake River (#5, Fig. 4.2). Lake Lyes, interpreted as a crown-scarp or "neck" pond in a large fault-controlled schist rockslide in the Whitcombe catchment [24], is also not considered here. Similarly, the Acheron rock avalanche (#19, Fig. 4.2) [30] is excluded from the dataset since it caused blockage of minor streams only. At three further omitted locations of former blockage on the Callery, Karangarua (McTaggart Ck), Moeraki (Horseshoe Flat), and Thomas (Haast) Rivers (#61, #49, #65, and #68, respectively, Fig. 4.2), rockslide-dam size could not be determined reliably.

3.2 Characteristics

The range of river-blocking rockslide and rock avalanche volumes lies between an arbitrarily set minimum of 10^6 m^3 and nearly 10^9 m^3. About half of the examined river-damming failures measure >1 km from scarp to toe and >2 km in runout, their average thickness being 30–40 m. At least 28 of them formed type II dams [4], and there are ten type III dams typical of rock avalanches. However, evidence of such additional tributary blockage was often more difficult to establish. Reliable estimates of dam height, H_D, and length, L_D, are available for about half of the sites, while dam width, W_D, could be determined for nearly 75% of the data (Table 4.1).

H_D ranges between 10 and ~400 m; with more than half of the dams being >50 m, and seven dams >100 m high. Irregular dam surfaces can create significant differences in H_D (Table 4.1). Mean L_D is 0.7 km, and mean W_D is 1.2 km. Only at two sites, i.e. Lochnagar and Hope Blue River Range, do L_D and W_D exceed 1.5 km and 2 km, respectively (Table 4.1). On average, rockslide and rock avalanche dams are more than 20 times as wide as they are high, thus forming very broad and often asymmetric cross-sections. This W_D/H_D ratio does not differ significantly with regard to failure type, i.e. rock sliding or avalanching, where one might expect higher ratios for catastrophic long-runout deposits. The total river length affected by a given dam, including backwater and downstream aggradation, is generally much longer, and may in few demonstrable cases reach up to 5 km [19]. Some of the dams were formed by large secondary debris flows fed by rockslide and rock avalanche debris, such as at Carls Ridge on Hendes Ck, Wanganui River (#59, Fig. 4.2).

Seven out of eleven available estimates on the volume of former rockslide-dammed lakes – mainly based on extrapolations of lake strandlines or lacustrine deposits [24] – exceed 10^7 m^3. Geomorphic evidence of smaller or ephemeral lakes is rarely reported. Absolute dates are available for 16 blockage sites. Six of these dams formed in historic times, with four during the 1929 Arthur's Pass earthquake alone [12]. Most of the remaining occurred during the late Holocene [30]. Trigger mechanisms for prehistoric dam formation remain speculative, although the spatial clustering of several rock-slope failures and river blockage strongly indicates regional triggering events [2, 24].

Only two of the rockslide and rock avalanche dams still retain lakes, of which Lochnagar in the Shotover catchment is the largest, with a lake volume of ~10^8 m^3[24]. Being alternatively interpreted as a rock avalanche [30] or rock-block slide [24], it is one of the largest river-blocking rock-slope failures in the study area (A_L >3.4 km^2; $V_L = 690 \times 10^6$ m^3), forming the highest intact dam (H_D ~340–400 m), although its exact size is disputed [24, 30] (#81, Fig. 4.2).

The only other rockslide-dammed lakes of comparable size in the South Island are Lake Christabel on Blue Grey River ($A_{Lake} = 2.6$ km^2), just north of the study area, Lake Constance ($A_{Lake} = 0.9$ km^2) in the North West Nelson Alps, and numerous others in the Fiordland mountains. The fact that these rockslide and rock avalanche dams remained so well preserved, may add bias to the geomorphometric

database, since erosion and deposition associated with failed dams may affect estimates of their original size.

Lake Minchin in the Poulter catchment [30] is the second-largest, presently existing lake dammed by a rock avalanche in the Southern Alps, covering an area of only 0.18 km^2 (#2, Fig. 4.2). There are no existing rockslide-dammed lakes west of the main divide. There, lakes are mostly ephemeral due to extremely high sediment yields which cause rapid infilling of both landslide- and glacially-dammed reservoirs in trunk valleys. Many of the rock avalanches in the ESA appear to have formed temporary dams, although geomorphic evidence of lake sedimentation is only found at 13% of the sites [30].

Several bivariate indices were used to empirically characterise "stability domains" for regional landslide-dam inventories [3, 17]. The low number of existing lakes in the Southern Alps precludes further testing of this approach. The majority of the rockslide and rock avalanche dams discussed here have not remained intact, and show evidence of breaching and fluvial erosion. Similarly to observed trends for New Zealand-wide data, the minimum deposit volume to retain a lake over several years or decades is estimated at 100×10^6 m^3 and 10^9 m^3, for 10 and 100-km^2 upstream catchment areas, respectively [17].

3.3 Distribution

Rockslide and rock avalanche dams occur on both sides of the main divide in similar numbers (Fig. 4.2). Although rock avalanches appear to be less frequent in the WSA [30], rivers there are blocked by large complex rockslides. Scatter plots show no significant differences in the relationships between deposit volume and dam dimensions on either side of the divide. Rockslide or rock avalanche volume V_L explains almost 60% of the (low) variance in dam width W_D. Dam height and length, H_D and L_D, respectively, may vary by over one order of magnitude for a given V_L (Fig. 4.3).

The majority of rockslide and rock avalanche dams occur in the upper reaches of alpine drainage basins with upstream catchment areas A_C <50 km^2, and only three blocked major channels (A_C >100 km^2). Similarly to dam geometry, there is no recognisable difference in this measure of relative catchment position between the western and eastern catchments of the Southern Alps. However, given generally smaller basin areas in the WSA, there, a river-blocking rockslide or rock avalanche of a given area A_L would be expected to affect a relatively larger portion of the catchment. This is reflected in the ratio A_L/A_C, which is on average 5% in the ESA, and 9% in the WSA.

3.4 Post-Failure Morphodynamics and Fluvial Adjustment

Most of the dams studied were breached. In many cases, breach channels evolved to steep meandering gorges cut through rockslide and rock avalanche debris, a

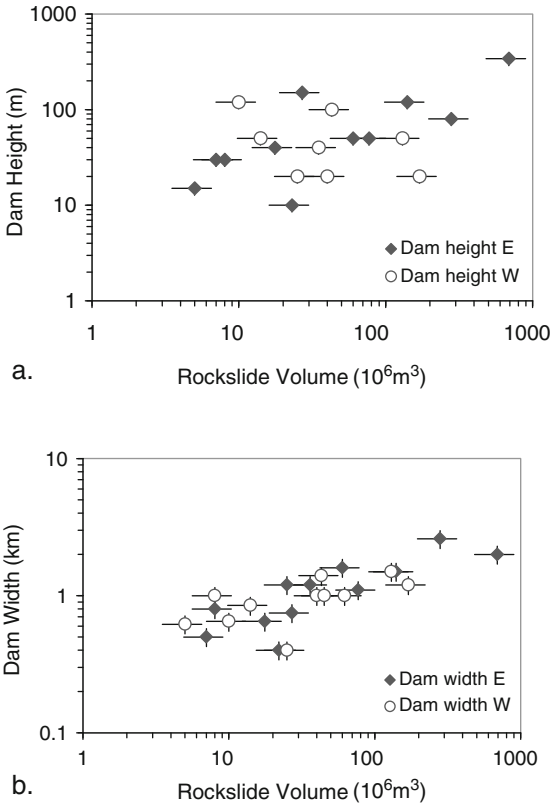

Fig. 4.3 Rockslide- (and rock avalanche) dam height H_D, and width W_D, as a function of rockslide volume V_L, for selected cases in the eastern (*black dots*) and western (*white dots*) Southern Alps. Bars allow for errors of ±30% and ±15% on *x*- and *y*-axes, respectively

characteristic which can aid visual reconnaissance from air photos. Impressive examples include the gorges at Falls Ck (160 m deep), below the Hope Blue River Range (200 m), and the Douglas River (120 m, Table 4.1). The "Zig–Zag" rock avalanche created a 55-m (at its highest point near the crest) to perhaps 130 m-high dam on upper Otira River, WSA, some 2,000 year ago (#8, Figs. 4.2 and 4.4a).

The dam impounds Pegleg Flat, forming a distinctive horizontal step ca. 0.8 km long and extending over 0.07 km^2. The river has cut a headward-eroding and 50–60-m deep gorge with an average gradient $S = 0.19$ through the debris (Fig. 4.5a). Geotechnical drilling conducted during the construction for a state highway viaduct through the rock avalanche deposition zone revealed that the bridge pylons required grounding in rock avalanche debris >30 m thick [25]. The Otira River thus has not adjusted to its former gradient since blockage occurred. Net fluvial downcutting along Pegleg Flat was as high as 0.1 m/year historically [18], and may be related to headward erosion at the dam crest.

This and other examples of breached dams allow insights into the state of fluvial recovery to blockage, assuming that the original channel gradient would have not had any major steps at the blockage site. For instance, the Polnoon Burn rockslide

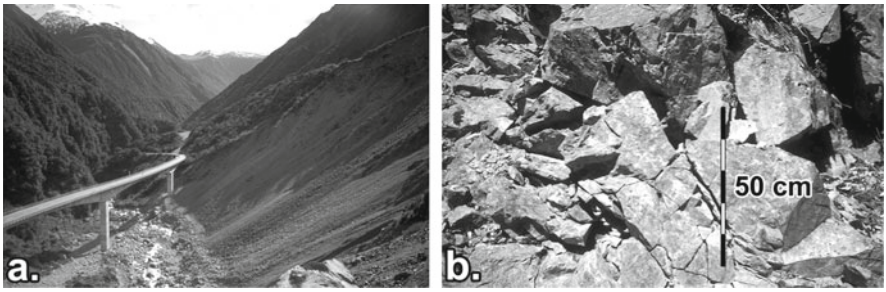

Fig. 4.4 Zig–Zag rock avalanche, Otira River, WSA. (**a**) Downstream view from the former rock avalanche dam crest at Death's Corner of the State Highway 6 viaduct located within the breach-channel gorge. Scree slope on the right is >100 m high and lower part of continuosly eroding rock avalanche debris. Note that bridge pylons are grounded in rock avalanche debris for >30 m. (**b**) Details of former roadcut in fragmented angular debris

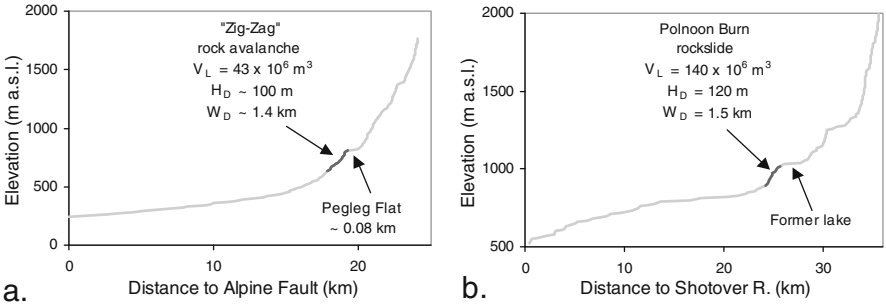

Fig. 4.5 Longitudinal profiles of **(a)** Otira River (WSA), and **(b)** Polnoon Burn (ESA). The ~2,000-year old "Zig–Zag" rock avalanche dam [30] continues to form a prominent step, with Pegleg Flat marking the extent of aggradation behind the dam. A similar step is evident in the upper Polnoon Burn

(A_L >1.9 km^2, $V_L = 140 \times 10^6$ m^3) in the Shotover catchment, ESA, formed a dam between 120 and 140 m high, judging from the depth of the present 1.7-km long river gorge dissecting the deposit (#82, Figs. 4.2 and 4.6).

The 4,000-year old dam [24] is ~1.2 km long and >1.5 km wide, forming a conspicuous >100 m high and slightly convex step in the river long profile. In the downstream section, this step is occupied by the breach channel ($S = 0.12$), while the flat upstream section results from backwater aggradation of ~3 km, representing the infilling of a former lake that lasted ~2,000 year [24] (Figs. 4.5b and 4.6). This knickpoint indicates that fluvial recovery at this site has also remained incomplete. The amount of rockslide debris eroded by the river is estimated between 20 and 40 $\times$ 10^6 m^3. With an upstream catchment area of 32 km^2, this would be equal to an average specific sediment yield between 2.8 and 5.6 $\times$ 10^2 t/km^2/year, while estimating bulk density at 1.8 t/m^3.

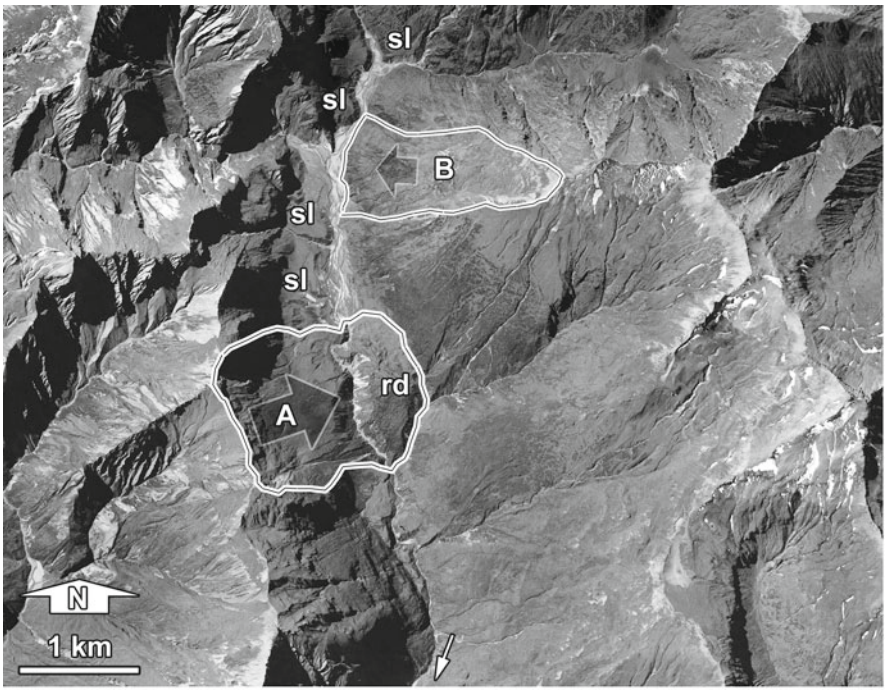

Fig. 4.6 Orthophoto of Polnoon Burn rockslide dam (rd), Shotover River, ESA. The rockslide originated from the western ridgeline (A), affecting >1.9 km^2, and damming the Polnoon Burn ~4,000 year ago [24]. The river has cut a meandering gorge through the deposit after a lacustrine phase that lasted some 2,000 year, evident in strandlines and level terraces (sl) (cf. Fig. 4.5b). Note that another 1.3-km^2 landslide (B) on the opposite upstream bank did not cause any obvious blockage due to low displacement. Image courtesy of Land Information New Zealand, Crown Copyright reserved (F40 Wanaka 2002/03, www.linz.govt.nz)

These figures may well be twice as high, if assuming that most of the dam erosion took place in the last 2,000 year, following the draining of the lake. Large bedrock landslides are prolific in the area. Another large ($A_L = 1.3$ km^2) complex landslide on the opposite bank just upstream did not cause any obvious blockage, possibly due to its low degree of displacement (Fig. 4.6).

In other cases, large cross-valley deposits appear to have been completely dissected, with the formerly dammed river having re-attained a profile gradient similar to that of its adjacent up- and downstream reaches. Some former breach channels thus have equilibrated to form broad gravel-bed rivers. This is for instance the case at the 2.6-km wide Boundary Ck rock avalanche dam ($V_L = 260 \times 10^6$ m^3; #23, Fig. 4.2), Mathias River, ESA, where the flat breach-channel floor is now ~200 m wide.

Similarly, the Cascade River, WSA, has cut a 3-km long and 200-m deep gorge through a catastrophic rockslide deposit below the Hope Blue River Range (#74, Fig. 4.2). The rockslide(s) affected ~9 km^2 and the debris is truncated by the Alpine

Fault trace, indicating a failure age >280 year, assuming that the fault was subject to surface rupture in this area in 1717 AD [29]. The eroded volume from the deposit is estimated at 130×10^6 m^3, theoretically resulting in a maximum sediment discharge rate of 4.6×10^5 m^3/year, or a specific sediment yield of 4,700 t/km^2/year.

Often, the results of river blockage are not as well-defined. High rates of erosion and deposition in the WSA make the identification of remnants of former rockslide and rock avalanche dams difficult. Also, several large rock-slope failures are associated with only minor impact on alpine rivers. This is exemplified in the Crooked River basin, where two large rockslides form a 20-m high type VI dam [4] (#57, #58, Figs. 4.2 and 4.7). The larger of the two ("Crooked A") is a complex failure, mobilising ~170×10^6 m^3, and extending over 3.7 km^2. A 300-m wide extensional scarp depression along the ridge crest exposes NE-trending schist foliation, and indicates failure along a schistosity plane with an estimated angle of $\varphi = 27° \pm 9°$. Compared to the total length of the failure (2.1 km), this scarp also shows that it has not moved very far. Steep ravines dissect and divide the failure complex into at least three individual slope portions. The maximum thickness of the rockslide exceeds 100 m, which is typical of many similar large-scale valley-side collapses in the WSA [30]. The rockslide is in direct contact with 1.8 km of Crooked River and 1.2 km of an unnamed right-hand tributary. Secondary slope failure(s) involving ~16×10^6 m^3 formed a debris fan, which has partly encroached onto the tributary junction ("df" in Fig. 4.7).

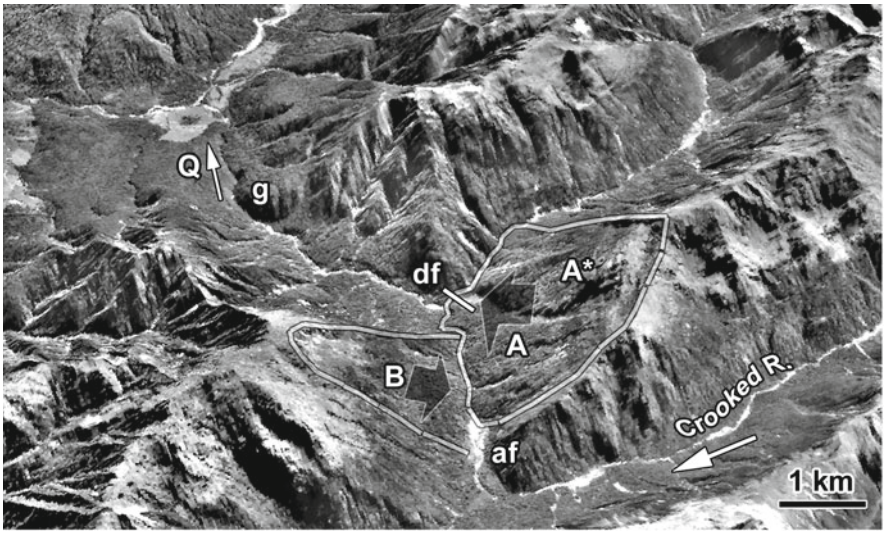

Fig. 4.7 Large rockslides (A: 170, and B: 40×10^6 m^3) forming a 20-m high type VI dam [4], and a small alluvial flat (af) on Crooked River, WSA. Note secondary failure scar (A*) and associated, partly trimmed, debris fan (df). Q = Quaternary glacigenic, fluvial, and debris-fan gravels cut by the Crooked R. gorge (g). View is to the north, scale approximate only. Image courtesy of Land Information New Zealand, Crown Copyright reserved (K32 Lake Brunner 1995/96, www.linz.govt.nz)

The "Crooked B" landslide is slightly juxtaposed and smaller (V_L = 40 to 50 × 10^6 m^3, with some 12 × 10^6 m^3 remaining as deposit on the lower slopes). Its motion may well have been triggered, or at least enhanced, by fluvial undercutting, following a possible initial channel diversion in response to the larger rockslide. Fluvial aggradation behind both landslides extends for up to ~1.2 km, forming a 0.3-km^2 intramontane alluvial flat fringed by forested terraces. The river longitudinal profile does not show any obvious step. The presence of knickpoints here is ambiguous, since they could also be the result of local channel adjustment at this major tributary junction.

Similar geomorphic impacts on river channels are common in the WSA, where large deep-seated rockslides have diverted river channels around their toes without creating persistent or well-defined blockage. At several such occlusion sites, fluvial trimming has oversteepened landslide toes, and triggered nested secondary rotational failures. Blockage of rivers by these secondary failures is interpreted to be mainly ephemeral and in close feedback with fluvial erosion, where no major obstructing deposits remain (Fig. 4.8).

3.5 Sediment Discharge

Once failed, rockslide and rock avalanche dams are subject to fluvial and mass-wasting erosion. Sediment discharge rates from eroding rock avalanches in the

Fig. 4.8 Downstream view of remnant of deep-seated rockslide (V_L ~22 × 10^6 m^3) on Dart River near Dart Hut (#78, Fig. 4.2), ESA (February 2001). Repeated rock-slope failure at this site may have caused short-lived river blockage several times

central Southern Alps lie between 10^2 and 1.5×10^5 m^3/year [30]. Averaged discharge from the breached 930-year old rock avalanche-dam on Jollie River amounts to 2.8×10^4 m^3/year or 7×10^2 t/km^2/year [30] (#46, Fig. 4.2), surpassing historically gauged catchment sediment yield by > 60%. Annual to decadal sediment discharge from failed rock avalanche dams may reach peak values of up to 1.8×10^6 m^3/year. Such specific yields are extreme (8×10^4 t/km^2/year), and were estimated in the months and years immediately following the failure of the 1999 Poerua rock avalanche dam below Mt Adams, WSA [19] (#52, Fig. 4.2). Such major sediment pulses can cause infilling of steep bedrock gorges and extend for several km downstream of the blockage site.

If extrapolated over longer periods (>1,000 year), the apparent average sediment discharge from eroding rockslide and rock avalanche dams is biased by formation age, though still ranges from 5×10^2 to 8×10^5 m^3/year. The highest specific yield from a prehistoric rock avalanche is 2.9×10^3 t/km^2/year (Boundary Ck, Mathias R.; #23, Fig. 4.2). These figures highlight the importance of rockslide and rock avalanche dams as major sediment sources in the Southern Alps, especially when considering, that over half of the studied failures affected only ~5% of their respective upstream catchment areas.

Predicting the sediment flux from breached rockslide dams would be useful for assessing the amount of consequential downstream aggradation on floodplains or alluvial fans. Although rockslide-dam height, assumed to be a proxy for hydraulic head, statistically explains 45% of the variation in mean specific sediment yield ($n = 10$), it is insensitive to the timing of delivery, which is indeed the most important aspect for hazard and risk assessments and river management. The breach of the Poerua rock avalanche dam demonstrated that sediment delivery was highest in the first months and years after the failure, and substantially declined afterward [19].

4 Discussion

4.1 Types and Occurrence of River Blockage

Review and compilation of geomorphic data from various sources sheds some new light on the distribution and characteristics of 43 rockslide and rock avalanche dams currently reported in the Southern Alps of New Zealand. A major finding is that evidence of river blockage occurs on both sides of the main divide in comparable numbers. Although this notion is open to further refinement due to the likely detection of additional former dam sites, it modifies earlier notions on the distribution and geomorphic impacts of rock avalanches in the WSA [30]. The 1999 Mt Adams rock avalanche, Poerua River, has shown the rapidity of dam erosion, and thus, removal of geomorphic evidence [19].

The geomorphic impact of rockslides and rock avalanches on alpine rivers is characterised by two distinctive types: (a) Rock-slope failures that produced clearly (and often catastrophically) detached deposits, which formed type II and

III dams [4]; and (b) Deep-seated, low-displacement, suspended or chronic, often sackung-type failures causing river diversion and occlusion around their toe zones. This type of landslide-induced river occlusion not always forms cross-valley barriers, though may involve ephemeral blockage through nested secondary rockslides or large surficial debris flows (Fig. 4.8).

There are several sites, where large rockslides or rock avalanches in direct contact with major channels did not produce any obvious effects of blockage. For instance, the Falling Mountain rock avalanche (V_L ~55 × 10^6 m^3), Otehake River (#5, Fig. 4.2), did not cause any major blockage, because it completely buried an alpine headwater branch.

Furthermore, several historic large rock avalanches also ran out on large glaciers, not causing any impact on the drainage system [22]. Several deep-seated complex rock-slope failures in schist lithology with volumes $\geq 10^8$ m^3 were not found to be associated with any blockage despite being located at the confluence of major rivers. The degree of displacement, velocity, and type of emplacement, are thus additional important controls on river blockage rather than the mobilised volume alone.

4.2 Regional Comparison

Assuming comparable numbers of occurrence on both sides of the divide, the geometry of rockslide and rock avalanche dams may be expected to reflect one or combined differences in external controls such as lithology, climate, valley geometry, or erosion rates. For instance, the runout of large rockslides and rock avalanches may be assumed to be less constrained by valley geometry in the trunk valleys east of the divide. The notion, that a given deposit volume, V_L, would thus produce a lower dam height, H_D, on average in the ESA, is not confirmed by the data (Fig. 4.3a).

Moreover, most of the mean geomorphometric characteristics of rockslide and rock avalanche dams are not strikingly different either side of the main divide. Dams have a slightly higher mean length, L_D, east of the main divide, possibly reflecting the influence of wider valley-floors on average. Differences in the mean or median width of dams, W_D, between the WSA and ESA, are however minute (i.e., <10%). This is interpreted as a result of fewer topographic constraints on dam formation in along-valley direction. Also, there is no detectable difference with regard to respective catchment location, as indicated by the contributing catchment area, A_C.

Extreme geomorphic process rates in the WSA constrain the longevity of rockslide-dammed lakes, and rapid dam-breaching or infilling is assumed. There, small contributing catchment areas and steep channels prevent the formation of large lakes, and high sediment yields shorten natural reservoir lifetimes to <100 year [8]. Process rates are one order of magnitude lower in the ESA, yet very few lakes are presently existing there. Judging from few published dates, these and other preserved large lakes north of the study area, may be ≥1,000-year old on average.

Comparison with the characteristics of numerous rockslide dams preserved in the Fiordland mountains highlights the controls of bedrock geology, seismicity, and sediment yield. There, large deep-seated rockslides have retained nearly 40 lakes [24]. Generally lower sediment yields [14] may explain the longer reservoir lifetimes. The higher rock-mass strength of the Fiordland crystalline basement implies, that deep-seated rock-slope failures require very high earthquake magnitudes to be triggered [10].

Thus an additional explanation for the better preservation of rockslide-dammed lakes in this region may be that of a fairly recent (nineteenth century) earthquake in the region [24]. The prominent glacial U-shape of many Fiordland valleys may also explain the better preservation of rockslide- and rock avalanche dammed lakes on broad and flat valley floors, although some of the valley fills may have also formed as a direct consequence of blockage.

4.3 Comparison with Other High Mountain Belts

A currently compiled inventory of 160 rockslide and rock avalanche dams in mountain belts throughout the world helps to put the geomorphic characteristics examined here into a global perspective. Scatter plots suggest that, for example, the relationship between dam height, H_D, and deposit volume, V_D, in the New Zealand Southern Alps does not differ much from those in other high mountain regions. The cases studied here occupy a "mid-field" position within the broad scatter of data collected from the European Alps, Central and High Asia, and the Andes, while any significant clustering is not evident (Fig. 4.9). Extremely large river-damming

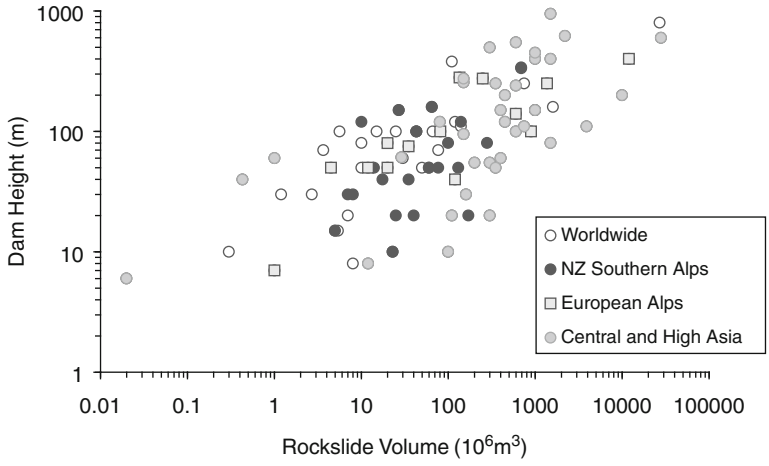

Fig. 4.9 Comparison of relationship between dam height, H_D, and deposit volume, V_L, for selected data from the New Zealand Southern Alps, the European Alps, Central and High Asia, and others. Data from the New Zealand Southern Alps take a "mid-field" position within the general scatter

rockslides ($V_L > 10^9$ m^3) or such that caused major drainage reversals are not documented in the study area. Site-specific conditions of blockage, such as e.g. valley geometry, lithology, climate, or deposit sedimentology subsumed in this scatter plot would need to be compared more directly in order to characterise regionally distinct types of rockslide and rock avalanche dams.

4.4 Implications for Trigger Mechanisms and Longevity

Judging from the number and area distribution of mapped landslides in the WSA, there may be a few hundred rockslides with volumes $>10^6$ m^3 in the Southern Alps, and it is likely that more rockslide and rock avalanche dams will be detected. More important however is the observation that many large rock-slope failures in the WSA do not show any geomorphic evidence of river blockage, either due to eradication of this evidence or close interaction between slope movement and fluvial erosion. Understanding better the dynamics of large-scale slope deformation is an important issue for future research, especially with regard to deep-seated sackung-type failures that are potentially subject to episodic or catastrophic reactivation by fluvial undercutting or earthquake shaking.

The next M ~8 earthquake on the Alpine Fault is likely to cause landsliding over some 10,000 km^2 of mountainous South Island terrain [12, 29]. Studies of historic New Zealand earthquakes illustrate the coseismic and synchronous formation of several rockslide dams. Thus the present situation of very few existing rockslide-dammed lakes may not be representative, given the short time it would take to obliterate evidence of such lakes, particularly in the WSA.

Assuming an age of ~1,000 year for the Lochnagar rockslide dam implies that the dam remained intact despite experiencing several major Alpine Fault earthquakes [29]. It remains speculative, whether repeated strong ground shaking has contributed to strengthening of the integrity of the dam. Unfortunately, little is known about the internal structure of rockslide dams until they are breached (Fig. 4.4b), although in many cases the sedimentologic characteristics of the dam govern its stability [28]. Intensely fragmented rock avalanche debris is much more prone to erosion than a coherent rock-block deposit, once the surficial boulder armour is breached. The longevity and size of dammed lakes on major rivers in the WSA may however be constrained more tightly by high sediment yields and river gradients, respectively.

There is also the possibility of spontaneous rock avalanching without any observed trigger [22], and deep-seated gravitational slope deformation (e.g. rock flow or sackung) acting as a precursor to catastrophic failure. The contemporary frequency of large rock avalanches in the ASA and ESA is estimated at 1 per 20–30 year [22], and this episodic river-damming potential should be regarded in addition to that from coseismic failures.

4.5 Long-Term and Long-Range Effects

The estimates of sediment discharge from rockslide dams in the Southern Alps confirm earlier observations [30], that large rockslides and rock avalanches are important (both prehistoric and contemporary) sources of sediment for alpine rivers. Reworking and temporary storage of eroded dam debris downstream can lead to adverse off-site effects of floodplain and fan-head aggradation, and channel avulsion, where agricultural land, infrastructure, or settlements are affected [18, 19]. Given a short transport distance and insufficient attenuation space, catastrophic sediment pulses pose lasting problems to land use and infrastructure, even several kilometres away from the actual rockslide or rock avalanche dam (Fig. 4.10).

Such long-term and long-range geomorphic effects necessitate the recognition of, and dealing with, a broader range of hazards from rockslides and rock avalanches. Experiences made with the Poerua rock avalanche dam give an indication of what

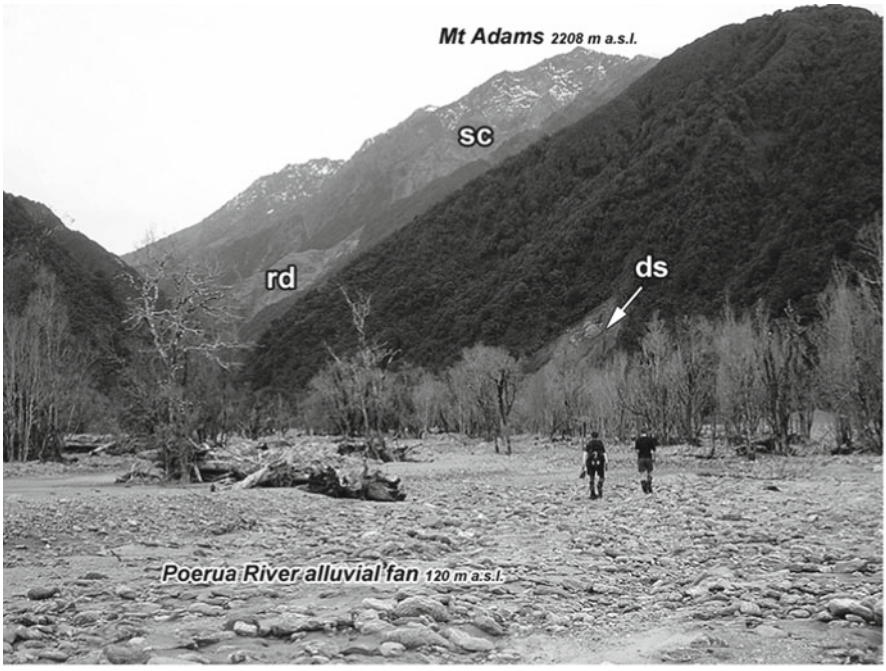

Fig. 4.10 Catastrophic aggradation is one long-term and long-range effect following the failure of rock avalanche dams, e.g. the >100-m high blockage (rd) below Mt Adams, Poerua River, WSA, in 1999 [11]. Sc = Scarp area; ds = secondary debris slide, induced by aggradation. Coarse sedimentation on Poerua River alluvial fan has buried pristine floodplain forests up to 6 m, with numerous dead trees remaining in growth position (photo taken by J. Thomson in March 2004, i.e. four-and-a-half years after dam failure)

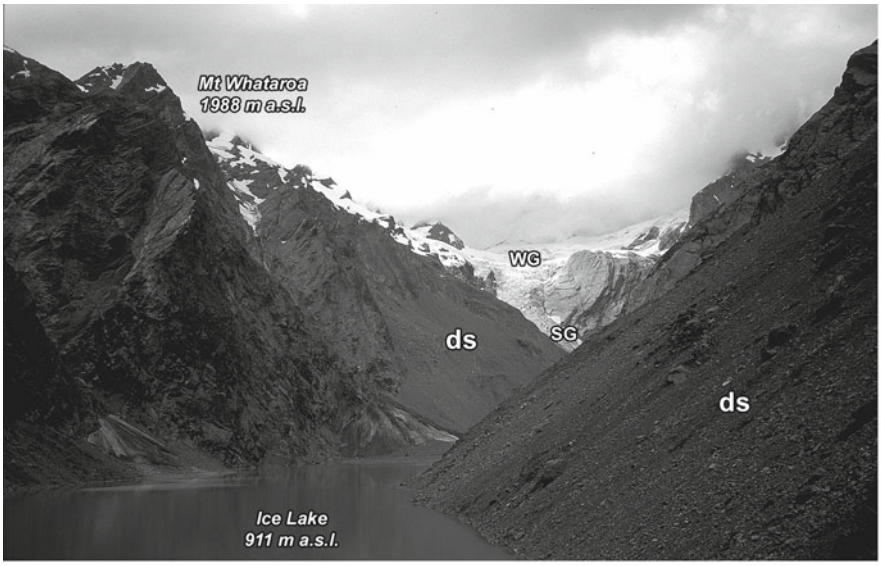

Fig. 4.11 Ice Lake on upper Butler/Whataroa River, near the main divide, WSA (March 2003). WG = Whataroa Glacier; SG = Shackleton Glacier. Instability on steep rock- and debris slopes (ds) may trigger landslide-induced displacement waves in this proglacial lake, potentially causing downstream flooding

to possibly expect at several locations, following the next major earthquake in the Southern Alps [11].

Similarly, rockslide and rock avalanche-induced displacement waves have not yet been addressed in detail in landslide (hazard) research in the Southern Alps. Rock avalanches from Mt Fletcher (1992), CSA, and a rockslide near Mt Aspiring (1988), have displaced millions of m^3 of water in proglacial lakes, causing downstream flooding [22]. Rockslide-dammed and proglacial lakes such as Ice Lake (Butler, Whataroa, WSA; Fig. 4.11), or several sites in the Mt Cook area (ASA, CSA) could give rise to displacement waves. However most of the lakes in question are situated in headwater areas at sufficient distances away from infrastructure or settlements, so that flood waves can attenuate, and a low destruction potential be assumed.

5 Conclusions

This study reviewed and compiled geomorphic evidence from 43 large ($>10^6$ m^3) river-damming rockslides and rock avalanches in the Southern Alps. A major finding is their occurrence in comparable numbers to the west and east of the main divide. Regional variations in lithology, precipitation, and valley geometry, are not particularly well reflected in geomorphometric characteristics of the dams. Catastrophic rock avalanches represent the dominant type of river-blocking slope failure in the greywacke terrain of the Southern Alps. In the schist lithology of

the western Southern Alps, evidence of river-damming rock avalanches is rarely observable. Instead, deep-seated complex failures with low displacement cause ephemeral blockage or, more prominently, channel occlusions and diversions. High rates of sediment yield and erosional processes constrain the longevity of rockslide- and rock avalanche-dammed lakes, of which very few presently exist. Given the currently high probability for a M ~8 earthquake [29], the present picture of rockslide- and rock avalanche impact on rivers in the Southern Alps may typify the final stage of alpine landscape recovery from episodic high-magnitude seismicity.

Post-failure morphodynamic processes of rockslide- and rock avalanche-dam decay can substantially extend the impact range of river blockage. Despite affecting small portions of a given catchment, the amount of debris supplied from breached dams can be massive, and even exceed catchment background yields for prolonged periods. Geomorphic consequences of catastrophic aggradation and channel instability pose persisting problems to downstream land-use, infrastructure, or settlements on floodplains and alluvial fans at the fringes of the Southern Alps.

The low population density in the New Zealand Southern Alps however keeps risk levels from direct rockslide or rock avalanche impact low. The piedmont west of the WSA is particularly vulnerable to outburst floods and post-failure aggradation from river-blocking rockslides and rock avalanches, where the short longevity of dammed lakes requires appropriate and rapid response immediately upon their formation. The broad and less steep valley trains of the ESA tend to reduce this potential by offering sufficient attenuation space.

Acknowledgements I thank the organizers of the 2004 Bishkek NATO ARW for their invitation to a very inspiring meeting. Thanks are also extended to R.L. Schuster, M. Crozier, N. Perrin, G. Dellow, T.R. Davies, M. McSaveney, and S.G. Evans for many encouraging discussions.

References

1. Adams, J.E. (1980) Contemporary uplift and erosion of the Southern Alps, New Zealand. Part 2, *Geological Society of America Bulletin* **91**, 1–114.
2. Bull, W.B. and Brandon, M.T. (1998) Lichen dating of earthquake-generated regional rockfall events, Southern Alps, New Zealand, *Geological Society of America Bulletin* **110**, 60–84.
3. Casagli, N. and Ermini, L. (1999) Geomorphic analysis of landslide dams in the Northern Apennine, *Transactions Japanese Geomorphological Union* **20**, 219–249.
4. Costa, J.E. and Schuster, R.L. (1988) The formation and failure of natural dams, *Geological Society of America Bulletin* **100**, 1054–1068.
5. Davies, T.R.H. (2002) Landslide-dambreak floods at Franz Josef Glacier township, Westland, New Zealand: A risk assessment, *Journal of Hydrology (New Zealand)* **41**, 1–17.
6. Davies, T.R. and McSaveney, M.J. (2002) Dynamic simulation of the motion of fragmenting rock avalanches, *Canadian Geotechnical Journal* **39**, 789–798.
7. Davies, T.R.H. and Scott, B.K. (1997) Dambreak flood hazard from the Callery River, Westland, New Zealand, *Journal of Hydrology (New Zealand)* **36**, 1–13.
8. Einsele, G. and Hinderer, M. (1997) Terrestrial sediment yield and the lifetimes of reservoirs, lakes, and larger basins, *Geologische Rundschau* **86**, 288–310.
9. Griffiths, G.A. (1979) High (suspended) sediment yields from major rivers of the Western Southern Alps, New Zealand, *Nature* **282**, 61–63.

10. Hancox, G.T., Cox, S.C., Turnbull, I.M. and Crozier, M.J. (2003) Reconnaissance studies of landslides and other ground damage caused by the M_w 7.2 Fiordland earthquake of 22 August 2003, *Institute of Geological & Nuclear Sciences Science Report* **2003/30**, 39 pp.
11. Hancox, G.T., McSaveney, M.J., Davies, T.R. and Hodgson, K. (1999) Mt Adams rock avalanche of 6 October 1999 and subsequent formation and breaching of a large landslide dam in Poerua River, Westland, New Zealand, *Institute of Geological and Nuclear Sciences Report* **99/19**, Lower Hutt, 22 pp.
12. Hancox, G.T., Perrin, N.D. and Dellow, G.D. (1997) Earthquake-induced landsliding in New Zealand and implications for MM intensity and seismic hazard assessment, *Institute of Geological and Nuclear Sciences Client Report* **43601B**, prepared for Earthquake Commission Research Foundation. Lower Hutt, 85 pp.
13. Henderson, R.D. and Thompson, S.M. (1999) Extreme rainfalls in the Southern Alps of New Zealand, *Journal of Hydrology (New Zealand)* **38**, 309–330.
14. Hicks, M., Shankar, U. and Mckerchar, A. (2003) Sediment yield estimates: A GIS tool, *NIWA Water & Atmosphere* **11**, 26–27.
15. Koons, P.O. (1989) The topographic evolution of mountain belts: A numerical look at the Southern Alps, New Zealand, *American Journal of Science* **289**, 1041–1069.
16. Korup, O. (2002) Recent research on landslide dams – a literature review with special attention to New Zealand, *Progress in Physical Geography* **26**, 206–235.
17. Korup, O. (2004) Geomorphometric characteristics of New Zealand landslide dams, *Engineering Geology* **73**, 13–35.
18. Korup, O. (2004) Landslide-induced river channel avulsions in mountain catchments of southwest New Zealand, *Geomorphology* **63**, 57–80.
19. Korup, O., McSaveney, M.J. and Davies, T.R.H. (2004) Sediment generation and delivery from large historic landslides in the Southern Alps, New Zealand, *Geomorphology* **61**, 189–207.
20. Little, T.A., Holcombe, R.J. and Ilg, B.R. (2002) Kinematics of oblique collision and ramping inferred from microstructures and strain in middle crustal rocks, central Southern Alps, New Zealand, *Journal of Structural Geology* **24**, 219–239.
21. Long, D.T., Cox, S.C., Bannister, S., Gerstenberger, M.C. and Okaya, D. (2003) Upper crustal structure beneath the eastern Southern Alps and the Mackenzie Basin, New Zealand, derived from seismic reflection data, *New Zealand Journal of Geology and Geophysics* **46**, 21–39.
22. McSaveney, M.J. (2002) Recent rockfalls and rock avalanches in Mount Cook National Park, New Zealand, in S.G. Evans and J.V. DeGraff (eds.), *Catastrophic Landslides: Effects, Occurrence, and Mechanisms*, Reviews in Engineering Geology **XV**, Geological Society of America, Boulder, CO, pp. 35–70.
23. Norris, R.J. and Cooper, A.F. (2000) Late Quaternary slip rates and slip partitioning on the Alpine fault, New Zealand, *Journal of Structural Geology* **23**, 507–520.
24. Perrin, N.D. and Hancox, G.T. (1992) Landslide-dammed lakes in New Zealand preliminary studies on their distribution, causes and effects, in D.H. Bell (ed.), *Landslides. Glissements de terrain*, Balkema, Rotterdam, pp. 1457–1466.
25. Ramsay, G. (2000) Otira Gorge rock avalanche, in E. Bromhead, N. Dixon and M.L. Ibsen (eds.), *Landslides in Research, Theory and Practice*, Thomas Telford, London, pp. 1274–1280.
26. Schuster, R.L. (2000) Outburst debris flows from failure of natural dams, in G.F. Wieczorek and N.D. Naeser (eds.), *2nd International Conference on Debris-Flow Hazard Mitigation*, Balkema, Rotterdam, pp. 29–42.
27. Tippett, J.M. and Kamp, P.J.J. (1995) Quantitative relationships between uplift and relief parameters for the Southern Alps, New Zealand, as determined by fission track analysis, *Earth Surface Processes and Landforms* **20**, 153–175.
28. Weidinger, J.T., Wang, J. and Ma, N. (2002) The earthquake-triggered rock avalanche of Cui Ha, Qin Ling Mountains, P.R. of China – the benefits of a lake-damming prehistoric natural disaster, *Quaternary International* **93–94**, 107–214.

29. Wells, A., Duncan, R.P., Stewart, G.H. and Yetton, M.D. (1999) Prehistoric dates of the most recent Alpine fault earthquakes, New Zealand, *Geology* **27**, 995–998.
30. Whitehouse, I.E. (1983) Distribution of large rock avalanche deposits in the central Southern Alps, New Zealand, *New Zealand Journal of Geology and Geophysics* **26**, 272–279.
31. Whitehouse, I.E. (1988) Geomorphology of the central Southern Alps, New Zealand: The interaction of plate collision and atmospheric circulation, *Zeitschrift für Geomorphologie NF* **69**, 105–116.